EPJ E
Soft Matter and Biological Physics
EPJ.org
your physics journal

Eur. Phys. J. E (2011) **34**: 112 DOI 10.1140/epje/i2011-11112-x

Effect of a capillary meniscus on the Faraday instability threshold

K.D. Nguyem Thu Lam and H. Caps

EDP SCIENCES
Società Italiana di Fisica
Springer

Eur. Phys. J. E (2011) **34**: 112
DOI 10.1140/epje/i2011-11112-x

THE EUROPEAN PHYSICAL JOURNAL E

Regular Article

Effect of a capillary meniscus on the Faraday instability threshold

K.D. Nguyem Thu Lam[1] and H. Caps[2,a]

[1] PMMH, École Supérieure de Physique et de Chimie Industrielles, 75231 Paris, France
[2] GRASP, Physics Department B5, University of Liège, B-4000 Liège, Belgium

Received 24 March 2011 and Received in final form 23 May 2011
Published online: 19 October 2011 –

Abstract. Threshold for Faraday instability has been experimentally measured for slightly viscous liquids. Changing the size of the container containing the fluid allows us to emphasize the role played by the capillary meniscus on the onset for instability. As the container is getting smaller, an upset of the critical acceleration is observed. Below a given container diameter, eigenmodes are observed along the stability curve. A dissipation term is proposed for considering the viscous dissipation against the walls of the container.

1 Introduction

Hydrodynamic instabilities have been widely investigated for many decades. Theoretical, experimental and numerical works have been performed in the aim of understanding the physical mechanisms responsible for the appearance of pattern and their transition to a disordered state. Among others, the case of the Faraday instability [1] received a special attention. This instability occurs when a liquid bath is vertically oscillated above a critical acceleration Γ_c. For acceleration values in the vicinity of Γ_c, the fluid/air interface is covered by a set of standing waves which can be ordered into different geometries like squares, concentric circles, triangles, spirals, etc. [1–6]. Above this linear regime, the patterns become unstable and chaos may appear [7]. Increasing higher again the driving acceleration causes the breaking of the waves and drop ejection may be observed [8].

Most of the papers on Faraday instability assume that either the liquid bath is spatially infinite or that the liquid surface is normal to the walls of the container at the triple line. In most of the experimental situations, this assumption is naturally not respected and different results are expected [5]. The particular case of miscible fluids has to be pointed out [9]. One of the effects of this non-normal connection is the generation of surface waves close to the side walls and, subsequently, an energy dissipation in the case of viscous fluids. As the system is shaken for producing Faraday waves, the apparent gravity varies, leading to an oscillatory dynamics of the meniscus length. In order to ensure mass conservation, surface waves are generated at the driving frequency. The dynamics of the meniscus in this oscillating regime is quite complex [10–12]. Moreover, such emitted surface waves interfere with the sub-harmonic Faraday patterns and their onset for appearance.

The present paper addresses this problem of Faraday waves generated at an interface having a non-normal connection angle with the walls of the container. The following experimental study concerns a viscous fluid inside a finite container. Attention is paid to viscous dissipation at the container walls, as a parameter influencing the onset for instability. Due to the emission of surface waves from the meniscus, an upshift of the threshold for instability is expected, which should depend on the contact angle.

2 Theoretical background

As the fluid bath is submitted to vertical oscillations, the free surface experiences deformations and surface waves appear. The latter can be described in terms of the vertical elevation of the free surface $z = \zeta(x, y, t)$. Considering that the wave amplitude is small compared to its wavelength, and that standing waves appear, the free surface elevation can be rewritten in terms of eigenmodes $S_m(x, y)$, such that

$$\zeta(x, y, t) = \sum_m \zeta_m(t)\, S_m(x, y). \tag{1}$$

Each of these modes can be modeled as a harmonic oscillator governed by

$$\ddot{\zeta} = -\omega_m^2 \zeta_m, \tag{2}$$

where ω_m is the natural frequency of the oscillator corresponding to the eigenmode m. This natural frequency obeys $\omega_m = \Omega(k_m)$, with each of the $\Omega(k)$ given by the

[a] e-mail: herve.caps@ulg.ac.be

following dispersion relation:

$$\Omega(k) = \left[\left(g_0 k + \frac{\sigma}{\rho}k^3\right)\tanh(kh)\right]^{1/2}, \qquad (3)$$

where k is the wave number corresponding to the mode m, g_0 is the gravitational acceleration and σ is the surface tension of the liquid. The external excitation imposed to the system can be seen as a temporal modulation of g_0, such that the liquid experiences

$$g(t) = g_0 - \Gamma\cos(\omega t), \qquad (4)$$

where $\Gamma = A\omega^2$, with A being the amplitude of oscillations and ω their frequency. It has been shown [13] that including this modulation into a linearization of the Euler equations still leads to eigenmodes, but parametrically excited. The free surface is now given by

$$\ddot{\zeta} = -\left[\omega_m^2 - (k_m\tanh(k_m h))a\cos(\omega t)\right]\zeta_m, \qquad (5)$$

where ω_m still obeys $\omega_m = \Omega(k_m)$. Faraday waves are therefore parametrically excited surface waves. Gravitational waves are generated when $g_0 k$ is larger than $\sigma k^3/\rho$. Otherwise, they are called capillary waves. As we will see further, all the measurements presented in the present paper are obtained close to the Γ_c threshold, within the capillary wave regime.

If the instablity is generated in a slightly viscous liquid, then, some mechanical energy is dissipated. As proposed in [14], this energy dissipation can be taken into account by adding a damping term to the previous linear theory. The damping coeficient γ_ν can be estimated by solving the ratio between the total mechanical energy of the system and the rate of energy dissipation,

$$\gamma_\nu = \frac{|\langle\dot{E}\rangle|}{2\langle E\rangle}, \qquad (6)$$

where the $\langle\ldots\rangle$ symbols stand for time averaging [14]. These energies read

$$E = \rho\int v^2\,\mathrm{d}V \sim \rho v^2(R^2k^{-1}) \qquad (7)$$

and

$$\dot{E} = -2\rho\nu\int(\nabla\cdot\mathbf{v})^2\,\mathrm{d}V \sim \rho\nu(v/k^{-1})^2(R^2k^{-1}), \qquad (8)$$

for a fluid of density ρ in a container of typical diameter $2R = d$ moving at a characteristic velocity v such that a wave number k is excited. Eventually, one gets

$$\gamma_\nu \sim \nu k^2. \qquad (9)$$

The inclusion of such a term has been addressed in various papers, among which [2, 15–17]. One of the advantages of this phenomenological approach is to preserve the non-coupling of the eigenmodes.

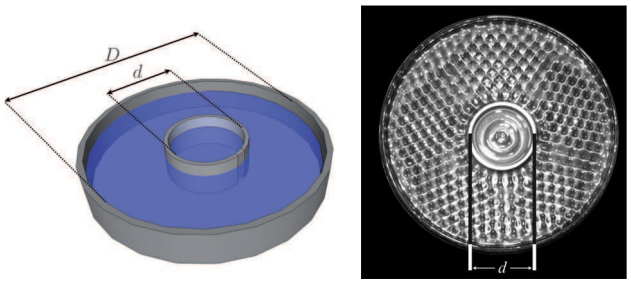

Fig. 1. Top view of the experimental container. Faraday instability is measured within the central circle having a diameter d.

Usually, such classical linear theories do not consider any geometrical confinement of the fluid, *e.g.* [17, 18]. When considering the finite size of the vessel, one has to suppose that the contact line between the fluid and the walls defines an angle θ. The ideal situation is met for $\theta = \pi/2$ when capillary effects at the walls can be neglected. For any other value of θ, the surface tension is responsible for the apearance of a capillary meniscus, whose spatial extension depends on $g(t)$. The interaction between Faraday waves and this time evolving meniscus is the main feature of the present paper.

3 Experimental set-up

The experimental set-up for producing Faraday instability is composed of an electromagnetic shaker receiving an oscillating voltage owing a given frequency f. The amplitude A of oscillations is accurately measured by means of a piezoelectric accelerometer fixed onto the vibrating table and giving the driving acceleration value $\Gamma = A\omega^2$, where $\omega = 2\pi f$. The fluid is a 10 cSt silicon oil ($\rho = 0.934\,\mathrm{kg/m^3}$, $\sigma = 0.0201\,\mathrm{N/m}$) and is contained into a cylindrical vessel (diameter $D = 20\,\mathrm{cm}$, height $h = 3\,\mathrm{cm}$) made out of pyrex. At the center of this vessel, a cylinder of diameter d made of aluminum is fixed and is considered as the experimental cell (see fig. 1). Changing the diameter of the experimental cell is thus fast and easy. A small hole (1 mm in diameter) has been drilled at the bottom of this small cylinder in order to allow the fluid to reach the same level in both containers. Since the fluid is viscous and the oscillations are of typically a few Hz, no fluid motion takes place into this hole. Moreover, the fluid level ($\sim 2.5\,\mathrm{cm}$) is large enough to ensure that the bottom plate can be assumed to have no effect on the surface instability onset ($kh \sim 1$). We have also verified that the contact line was not moving during the experiments, ensuring that no hysteresis of the contact angle has to be accounted for.

The threshold of the instability has been measured by increasing the driving acceleration in steps at a constant frequency value. A stroboscopic LED light was connected to the signal generator for helping in determining when the sub-harmonic regime is reached.

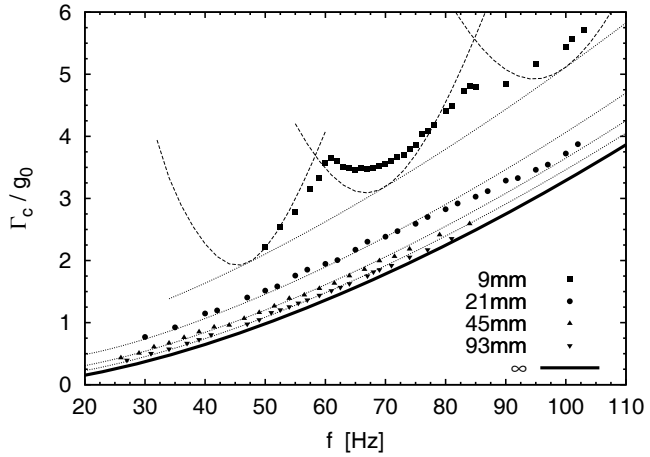

Fig. 2. Normalized critical acceleration Γ_c/g_0 for Faraday instability as a function of the forcing frequency f. Experimental data corresponding to different container diameters are presented, as black symbols. Dashed and solid lines are numerical modeling including damping coefficients of eqs. (9) and (12).

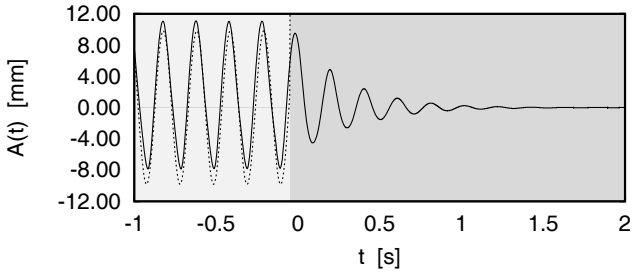

Fig. 3. Wave amplitude as a function of time for Faraday waves in water. The natural mode $m = 2$ (eq. (1)) is excited ($t \leq 0$) and then left at rest. The damping of the free surface waves is observed for $t \geq 0$. The dashed sinusoidal curve oscillates at the free wave regime frequency observed for $t \geq 0$ and slightly differs from the forcing frequency.

4 Onset for instability

The onset for instability has been measured for different container diameter values within the range $9 \leq d \leq 93$ mm. Data points corresponding to four d values are presented in fig. 2. It can be seen that, as the diameter d decreases, an upshift of the threshold is observed. In the case of the smaller container, lobes are observed and correspond to the resonance of the free surface. These modes have been identified and are the same as those expected for an inviscid fluid. Due to surface tension, they are however decorated with a non-normal connection at the side walls, as predicted in [19]. It should be noted that the transition between successive modes is smooth. This is somewhat surprising since the capillary meniscus sometimes extends to more than half the cylinder surface.

Decreasing the size of the vessel results in a growing relative effect of the capillary meniscus at the walls. Due to the external forcing, the characteristic height of this meniscus is evolving as $\ell = \sqrt{\sigma/\rho g(t)}$ [19]. In order to ensure mass conservation, this modification of the meniscus volume leads to the emission of capillary waves, at the forcing frequency f. Viscosity is responsible for the damping of these waves. Recalling eq. (9) for the damping coefficient due to viscosity, one sees that the waves travel a typical distance $v{\gamma_\nu}^{-1}$ at a characteristic velocity $v = \omega/2k$, during a time ${\gamma_\nu}^{-1}$. The length of the meniscus is thus of the order of $l \sim \omega/\nu k^3$ which reads, in the capillary wave regime, $l \sim \sigma/4\rho\nu\omega$.

As previously for the viscosity, we will suppose that a phenomenological term can be added to the linear theory for modeling this capillary effect due to the geometrical confinement. In agreement to the non-slip condition at side walls of the vessel, we assume that the vertical component of the velocity experiences a gradient within a boundary layer having a thickness $\delta = \sqrt{\nu\omega^{-1}}$. The energy loss can be modeled by the mechanical balance energy eq. (6), giving

$$E \sim \rho v^2 (R^2 k^{-1}) \tag{10}$$

and

$$\dot{E} \sim \rho\nu (v^2/\delta^2)(Rk^{-1}\delta). \tag{11}$$

The damping coefficient, γ_σ corresponding to the energy dissipation at the wall is thus given by

$$\gamma_\sigma = \omega \frac{\delta}{R}. \tag{12}$$

The solid curve of fig. 2 presents theoretical predictions based on the linear theory including the γ_ν damping coefficient, while the dashed lines correspond to this theory, including the energy dissipation in the vicinity of the container by means of γ_σ. These theoretical predictions are superimposed to experimental results. It should be noted that the order of magnitude estimate of γ_σ, as written in eq. (12), has been multiplied by an empirical numerical pre-factor 1.25, allowing a quantitative agreement between experiments and theory. For the smallest container ($d = 9$ mm), a larger deviation from experimental data is however observed. The strong coupling between Faraday waves and the waves generated by the meniscus, at the forcing frequency, could be considered as the source of this dissension. In such a small container, capillary waves nearly extend all over the free surface.

In order to validate the introduction of the γ_σ coefficient in the linear theory, we performed damping measurements of the Faraday waves. The free surface was oscillated in such a way that one of the first symmetric modes was excited, namely $m = 2$. Working with small mode numbers allows for large k numbers and large wave amplitudes. Figure 3 presents a typical run for a container filled with water. The wave amplitude $A(t)$ is plotted as a function of time. This figure was obtained by imaging an illuminated sheet of the free surface with a high-speed video camera at a frame rate of 2000 frames per second. The video camera was then tilted in order to record, from above, the shape of the light sheet on the deformed free

surface. The oscillations are stopped at the time $t = 0\,\mathrm{s}$. The asymmetry in the wave amplitude is due to the nonlinearity of the waves which are higher than deep, with respect to the reference position [20]. After the forcing oscillations are stopped, the free surface waves regime commences. The wave frequency is changing due to this new regime and the wave amplitude is damped. The difference between the forcing frequency and the free one can be seen in fig. 3 where the non-damped free surface wave oscillation (dashed line) is superimposed to the forcing signal for $t \leq 0$. Fitting a modulating exponential decay on the curves for $t \geq 0$ gives the damping coefficient γ_σ. In fig. 3, the obtained value is $\gamma_\sigma = 3.52 \pm 0.06\,\mathrm{s}^{-1}$. Recalling the order of magnitude estimate for the bulk viscous dissipation, $\gamma_\nu \sim \nu k^2 \sim 0.01\,\mathrm{s}^{-1}$, one sees that the wall contribution is quite large. Now recalling eq. (12), one obtains $\gamma_\sigma \sim \omega\delta/R \sim 1\,\mathrm{s}^{-1}$. This estimate gives the good order of magnitude for the damping coefficient.

Based on this γ_σ value, we can theoretically estimate [6] the critical acceleration to $\Gamma_c = 0.489 g_0$. Experimentally, we measured $\Gamma_c = 0.49 \pm 0.005 g_0$, in very good agreement with the prediction. For all the experiments we performed, a quantitative agreement has been noticed between experimental results and theoretical predictions including the measured damping coefficients.

This result justifies the use of a damping term within a linear theory in order to model the viscous dissipation due to meniscus waves.

5 Contact angle

As it is emphasized above, the viscous dissipation in the boundary layer plays an important role in the destabilization threshold of the free surface. It is usually assumed (theoretically) or forced (experimentally) that the triple line is pinned in such a way that the connection of the fluid on the container is normal. When this brimfull condition in not met, the capillary meniscus is expected to change the spatial extension δ of the velocity gradient. The latter should indeed be larger. In order to check this assumption, we have measured the threshold for Faraday instability for different configurations of the meniscus. We started from a situation where the meniscus if fully developed and the triple line is touching the top of the container. We have then increased the amount of liquid inside the container, still forcing the contact line to be pinned. This progressive filling resulted in a continuous variation of the spatial extension of the capillary meniscus, passing by the normal connection configuration (brimful condition).

Due to the circular geometry of our set-up, it is rather difficult to measure the contact angle. We thus solved the Laplace equations for the meniscus [14] in order to deduce the contact angle. We imposed the horizontality of the free surface at the center of container, knowing that the height of the free surface is given by the amount of liquid added into the container. In fig. 4, the normalized critical acceleration Γ_c/g_0 is plotted as a function of the amount of added liquid ΔV. The corresponding contact angles are given in the top part of this figure. It should be noted that

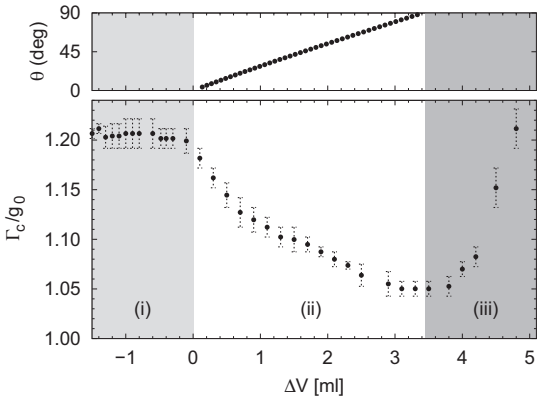

Fig. 4. Top: apparent contact angle at the meniscus as a function of the added volume ΔV inside a vessel of diameter 45 mm. Bottom: threshold for Faraday instability ($f = 50\,\mathrm{Hz}$) as a function of ΔV. Three regions can be distinguished (see text for further details).

we also explored the effect of removing some liquid (noted as $\Delta V \leq 0$).

For small liquid contents (*i.e.* $\Delta V \leq 0$, region (i) of fig. 4), the threshold is constant. As we remove the liquid from the container, the contact angle is still very small (silicon oil in contact with glass) and does not vary, allowing a full development of the capillary meniscus. For all the values of $\Delta V \leq 0$ we tested, the depth of the liquid enters the infinite depth approximation, explaining this result.

As we pour liquid, 0.1 ml by 0.1 ml, the contact line remains pinned on the container border (region (ii) of fig. 4). Increasing further the amount of liquid leads to an increase in the contact angle. It is observed that the critical acceleration Γ_c reaches its minimal value when the free surface is horizontal, *i.e.* when the contact angle is $\pi/2$. This minimum occurs for $\Delta V \approx 3.5\,\mathrm{ml}$. Knowing the exact geometry of the vessel and considering the pinning of the contact line, the expected value is $\Delta V \approx 3.47\,\mathrm{ml}$. The measured value for Γ_c is very close to the expected value for a viscous infinite fluid, emphasizing the relevance of this simple technique for varying the apparent contact angle and the subsequent meniscus wave extension.

Adding more liquid into the container leads to an increase in the threshold for instability (region (iii) of fig. 4). For these measurements, an overflow was observed, very small at the beginning but significant for large ΔV values. At the container walls, the critical acceleration is thus going out of the infinite depth approximation and the Faraday waves are damped. The resulting increase in Γ_c was previously observed and reported in [21].

6 Conclusions

Both the size d of the container and the contact angle θ modify the critical acceleration Γ_c. With respect to the infinite bath configuration, a larger value of Γ_c is measured as soon as d takes a finite value. Any deviation of θ from

the normal wetting condition (*e.g.* $\theta = \pi/2$) also results in a larger value of the critical acceleration. Those observations reveal that an increase of energy is required for inducing Faraday waves on a free surface where meniscus capillary waves generation is allowed. While the meniscus waves are harmonically generated, the Faraday ones are sub-harmonic. The interaction between these two kinds of waves thus has a stabilizing effect on the free surface. While decreasing d increases the relative spatial extension of the meniscus waves, modifying θ tunes the characteristic length of the capillary meniscus.

7 Summary

We have generated Faraday instability at air/liquid interfaces with different boundary conditions. The experimental results evidence the role played by the capillary meniscus on the threshold for instability. Depending on the spatial extension of this meniscus, different critical acceleration values are observed, for the same excitation parameters. Introducing a phenomenological term of viscous dissipation within a linear theory allows us to quantitatively describe the observed upshift in the critical acceleration.

The authors kindly acknowledge N. Vandewalle, T. Gilet and S. Dorbolo for fruitful discussions. Part of this project has been financially supported by Belspo-Prodex Program and by ESA Map Contract no. AO-99-108.

References

1. M. Faraday, Philos. Trans. R. Soc. London **121**, 299 (1831).
2. H.W. Müller, Phys. Rev. Lett. **71**, 3287 (1993).
3. W.S. Edwards, S. Fauve, J. Fluid Mech. **278**, 123 (1994).
4. D. Binks, W. van de Water, Phys. Rev. Lett. **78**, 4043 (1997).
5. S. Douady, S. Fauve, Europhys. Lett. **6**, 221 (1988).
6. W.S. Edwards, S. Fauve, J. Fluid Mech. **278**, 123 (1994).
7. A. Kudrolli, J.P. Gollub, Physica D **97**, 133 (1996).
8. C.L. Goodridge, H.G.E. Hentschel, D.P. Lathrop, Phys. Rev. Lett. **82**, 3062 (1999).
9. F. Zoueshtiagh, S. Amiroudine, R. Narayanan, J. Fluid Mech. **628**, 43 (2009).
10. J.W. Miles, Proc. R. Soc. London, Ser. A **297**, 459 (1967).
11. J.W. Miles, J. Fluid Mech. **245**, 485 (1992).
12. M. Perlin, W.W. Schultz, Annu. Rev. Fluid Mech. **32**, 241 (2000).
13. T.B. Benjamin, F. Ursell, Proc. R. Soc. London, Ser. A **225**, 505 (1954).
14. L. Landau, E. Lifchitz, *Mécanique des fluides* (Mir, Moscow, 1971).
15. M. Perlin, W.W. Schultz, Annu. Rev. Fluid Mech. **32**, 241 (2000).
16. K. Kumar, L.S. Tuckerman, J. Fluid Mech. **279**, 49 (1994).
17. K. Kumar, Proc. R. Soc. London, Ser. A **452**, 1113 (1996).
18. H.W. Müller, Lect. Notes Phys. **503**, 45 (1998).
19. S. Douady, J. Fluid Mech. **221**, 383 (1990).
20. J.V. Wehausen, E.V. Laitone, *Encyclopediæ of Physics*, Vol. **9**: *Surface waves in Fluid Dynamics III* (Springer-Verlag, 1960).
21. A. Eddi, E. Fort, F. Moisy, Y. Couder, Phys. Rev. Lett. **102**, 240401 (2009).